

Raman Analysis of Microplastics in Marine Litter

Matthew D. Kowal*

Department of Chemistry, The University of British Columbia

Vancouver BC, Canada, V6T 1Z1

Dr. Edward Grant Research Group

February 13, 2021

E-mail: mdkowal@chem.ubc.ca

Abstract

Raman serves to chemically identify microplastics. Microparticle samples, collected from zooplankton, larval herring, juvenile herring, and from the water column provide a baseline of marine litter in Baynes Sound near Vancouver, British Columbia, Canada. A Raman spectrum obtained for each sample served to identify it from a library of known materials based on a the dot product algorithm. One third of the samples were found to be synthetic in origin, one third were found to be of natural origin and one third failed to yield an identifiable signal.

1. Introduction

1.1. Context

Human beings have created an estimated 8 billion tons of plastic since inventing this class of substances 100 years ago. A small fraction of this remains sequestered in long-term use products such as machinery and building materials, but 76% of all the plastic we've ever made has been discarded as waste.¹ A small fraction of this waste may have been recycled or incinerated for energy generation but the bulk of it remains in landfills and the environment. At one time, plastics were celebrated as a wonder-material owing to their durability and chemical inertness, but now, recognizing that their material life, long-outlasts their useful product life they have become a blight on our planet. Plastic litter has formed a common sight on our beaches and elsewhere in the environment for decades, but at the small end of the particles size scale, microplastics have garnered increasing attention due to their overwhelming presence in the environment and their poorly understood effect on fauna. Microplastics have been found in oceans, lakes, soils^{2 3} air,⁴ and animals,⁵ as well as food⁶ and drinking water.⁷ Microplastics have become so ubiquitous in the environment that it has been suggested to use their presence as a geological indicator of the Anthropocene.⁸ Presumably, the only thing preventing us from finding microplastics in any location on earth is our ability to detect and measure them.

Early in the study of marine anthropogenic litter, the breakdown of plastics into smaller particles was considered natural and of little consequence.⁹ It is now known that micro and nanoplastics present a new and different set of dangers compared to macroplastics. Nanoplastics form vectors for plasticizers and other additives, and they present a huge surface area for the adsorbention of toxic chemicals.¹⁰ It has been shown that animals can mistakenly ingest microplastics as food, thus furnishing a conduit for the ingestion of toxins.⁶ Evidence suggests the trophic transfer of microplastics up the food chain from algae through zooplankton

to fish and birds.¹¹ Microplastics have also been found in store-bought seafood.⁶

Microplastics are defined to be any plastic particle less than 5mm in diameter.¹² There is no lower size limit for microplastics, although it has been suggested that particles $< 0.1 \mu\text{m}$ should be labeled as nanoplastics.¹³ Microplastics can enter the environment from many different sources. If they enter the environment as micro-sized particles they are considered primary microplastics and if they result from the breakdown of larger plastic waste they are considered secondary microplastics. Some examples of primary microplastics include plastic pellets used in industry (nurdles), synthetics clothing fibers,¹⁴ and glitter used in make-up and arts & crafts projects. Some examples of secondary microplastic sources are the breakdown products of fishing nets, plastic bags, food wrappers and packing materials. Although the mechanisms of plastic fragmentation are not fully understood, the major processes are presumed to be UV light and the frictional effects of waves.¹⁵ One study has found that Arctic Krill can even break down microplastics into nanoplastics.¹⁶

Little is known about the smallest sizes of micro and nanoplastics because they are so difficult to detect and measure. Several methods can serve to detect, quantify, and identify microplastics but each one has some drawbacks. Microscopy and visual identification commonly serve to identify large microplastics.¹⁷ But such methods become unreliable as particle size decreases. Optical techniques cannot distinguish between micron-sized natural and synthetic materials, and nanometer sized objects are entirely unresolvable. Electron microscopy can be used to observe nanoplastics,¹⁸ but the lack of chemical specificity and laborious sample preparation limit the scope of its applications. Elemental analysis may be used in conjunction with electron microscopy;¹⁹ however, without structural information it is impossible to determine the material origin of detected carbon atoms. In short, visual identification must be supplemented by chemical information in order to confidently determine the identity and source of anthropogenic marine litter.

Raman spectroscopy has served widely as a technique for chemical identification of microplastics. It is well suited for microplastics because it is easily integrated into a conventional

microscope, allowing morphological and chemical information to be obtained simultaneously, with no need for complicated sample preparation. Furthermore, Raman microscopy can detect a spectrum from particles as small as $1\mu m$. A typical Raman spectrum takes only seconds to acquire, and the identification can be easily automated. Once spectra have been collected it takes just minutes to identify hundreds of samples. This paper discusses the chemometric methods used in the automatic Raman identification of microparticle samples obtained in Baynes Sound, British Columbia, Canada.

1.2. Raman Fingerprinting for Microplastic Identification

1.2.1. Raman Fingerprint

The Raman spectrum for each material is unique and a well trained technician can in principle identify any common plastic type. But visual identification is a slow process when many samples are involved and opinion is susceptible to error, so a need exists to find faster and more reliable methods for chemical identification by Raman spectroscopy. The use of a Raman spectrum as a chemical fingerprint demands the consideration of several factors. Performing a search and match scheme requires a large database of labelled reference spectra. Comparing spectra from different spectrometers demands calibration of the spectra's wavenumber range and resolution. Low signal noise and background fluorescence also require corrections. Once these issues have been addressed, the peaks of interest can be isolated and matched to a database. Inconsistencies can slow down the visual identification of Raman spectra, but when treated algorithmically a set of signal processing techniques can quickly calibrate and compare many spectra very quickly.

1.2.2. A Large Database is Needed

A spectral identification algorithm requires a matching, known, and labelled spectrum for proper identification. The algorithm demands known spectra, forming a library, for all materials one expects to encounter in a sample-set. The most robust database would rely on the same spectrometer for both library and unknown samples. Furthermore, such a database should contain all possible chemical compositions including small modifications such as addition of dyes and variations in morphology. Each spectrum should be free of background fluorescence and noise. Such a database would have no errors in the labelling of the spectra and ideally have several levels of categorization for each material for the purpose of later discussion. Unfortunately, no one can make a perfect database, however these criteria make a useful target to aim for.

The present work uses a combination of three databases to identify microplastics. We created a primary database by taking Raman spectra of known plastics on our own Raman system. These plastics were sourced from packaging materials and clothing fibers. In total this database consisted of 13 materials from both natural (e.g. cotton) and synthetic (e.g. Polyethylene) origin. Many common polymers were missing from this database so it was supplemented with the SLoPP and SLoPP-E databases.²⁰ The SLoPP and SLoPP-E databases are publicly available Raman libraries made specifically for microplastics research by the Rochman Lab at the University of Toronto. The libraries contain 261 spectra of 15 different polymers with varying levels of environmental degradation.

1.2.3. Resampling

Spectra produced from different Raman Spectrometers produce signals of varying wavenumber ranges and spectral resolution, determined by spectrometer hardware and software settings used in acquisition. In order to compare spectra of different shapes they must first be calibrated to contain the same number of data points (range) with consistent data point spacing (resolution) between samples. We wrote a resampling algorithm in Python to quickly process all spectra before comparison. The resampling algorithm inserts regularly spaced data points into the spectrum, determining intensity values by interpolation of the nearest neighbors. This produces an oversampled spectrum. This algorithm then removes all irregularly spaced datapoints producing spectra with uniform wavenumber resolution. Finally, the regularization process trims the ends of each spectrum, standardizing the spectral range of the sample-set. (Fig. 1 A).

1.2.4. Noise Reduction

Noise is inherent in all real signals and cannot be avoided, but it can be managed, given some knowledge about the nature of the noise. If the noise frequency is expected to be significantly higher than the signal frequency then one can transform it to the frequency

domain, remove it mathematically, then reconstruct the spectrum (Fig. 1 B). The method of Fourier transform offers a suitable technique for transforming a signal into frequency domain. Discrete Wavelet Transform (DWT) allows one to choose the shape of the wavelet to match the wavelet shape of the signal. We have chosen to use the “sym5” wavelet because its shape best represents the shape of a Raman peak.

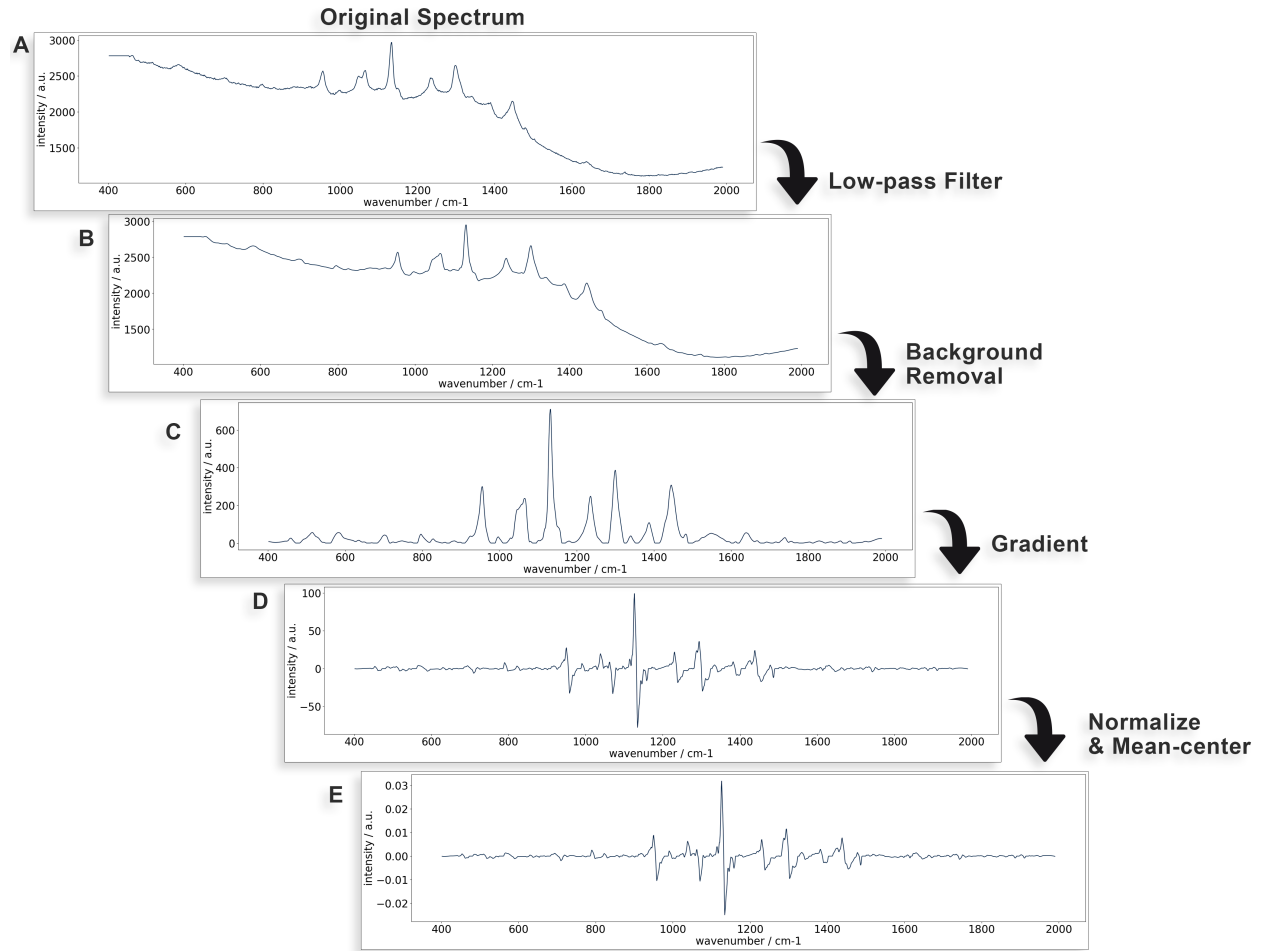


Figure 1: Standardization of a Raman spectrum during each step of the peak isolation algorithm. (A) Original Raman Spectrum after resampling. (B) Raman spectrum after high frequency noise removal. (C) Raman spectrum after fluorescent background removal. (D) Second derivative of the Raman spectrum. (E) Raman spectrum after L2 normalization and mean-centering.

1.2.5. Fluorescent Background Removal

Raman spectra often exhibits fluorescence as an intense, broad (low frequency) background that can greatly exceed the intensity of the Raman signal. Fluorescence occurs when the Ra-

man excitation energy drives an electronic transition in the sample. Removing the fluorescent background requires greater effort than removing noise, but DWT selection for the lowest frequency provides an estimate of fluorescence and removes it using an iterative method.²¹ This approach begins by deconstructing the spectrum into its lowest frequency components. We then estimate each data point of the background as the smaller value of either the original spectrum or its low frequency deconstruction. Feeding the estimated background back into the algorithm yields a new spectrum which increasingly approximates the fluorescence with each iteration. Repeating this process several times returns a well estimated background to then subtract from the original spectrum giving a new spectrum with a flat background (Fig. 1 C).

1.2.6. Peak Isolation

At its ultimate level, a Raman fingerprint matches the location and intensity of every Raman peak in a spectrum to those in a labelled set of reference spectra. Accurate matching requires a reliable pre-processing step to isolate Raman peaks from the background. The second derivative spectrum isolates peaks of interest by further flattening weak and broad background signals while accentuating sharp and well resolved Raman peaks (Fig. 1 D). After calculating the second derivative L2 normalization followed by mean-centering yields a standard bar-code-like signature (Fig. 1 E).

1.2.7. Finding A Best Match

Computers store and manipulate a Raman spectrum as a row vector. Thus digital signal processing techniques operate accordingly to best identify a sample based on an inventory of labeled spectra. Two identical vectors present an angle of 0 radians between them while two different vectors are almost always orthogonal in high dimensional space. The dot product describes this relationship and can be rearranged to solve for the angle θ (Eq. 1).

$$\theta = \arccos \frac{AB}{\|A\| \|B\|} \quad (1)$$

Theta is the angle between row vectors (spectra) A and B. Calculating the angle between a sample spectrum and each library spectrum, one can easily identify the library entry with the smallest angle as the best match. Using this method provides a best match for every sample spectrum, even when the best match does not represent a good fit, so a threshold must be applied to remove poor matches. A spectrum with a large angle between its best match will be considered a poor match with no positive identification.

1.2.8. Error Checking Using Signal to Noise Ratio

Sometimes, when a signal is weak, the peak isolation scheme can amplify noise and cause spurious matches with one of the reference spectra. Such a false positive happens rarely. The signal-to-noise ratio (SNR) can serve as a criterion to remove these types of false positives. The signal to noise ratio (Eq. 2) measures the intensity of signal peaks relative to the random background noise inherent in all measurements.

$$SNR = \frac{\max - \min}{\sigma} \quad (2)$$

The ratio of the total signal amplitude, $\max - \min$, to the standard deviation, σ , gives a measure of the meaningful signal. Many different formula exist for calculating signal to noise ratio. A choice of the correct formula is crucial for separating meaningful signals from meaningless ones. A more common formula is $SNR = \frac{\mu}{\sigma}$, where μ is the signal mean, and σ is the standard deviation. This formula is suitable for baseline corrected samples with L2 normalization, but for the algorithm used in this study, where the mean is set to zero, this formula returns zero SNR for all samples. Hence the reason for choosing equation 2.

2. Methods

2.1. Marine Litter Sample Collection and Preparation

Microplastics were collected by Brian Hunt's lab at the University of British Columbia Institute for the Oceans and Fisheries. Microplastic samples were isolated using standard protocols for microplastics research. Briefly, water samples were collected from 11 stations in Baynes Sound, British Columbia, Canada. A Niskin Bottle collects water samples from different depths in the water column then transferred to a glass carboy and sealed immediately to minimize contamination. Samples were also collected from dissection of Zooplankton, Larval Herring, and Juvenal Herring. In a laboratory clean room, samples were vacuum filtered onto a $10 \mu m$ polycarbonate filter using a glass funnel. The residue remaining on the filter membrane was added to 10% KOH solution and left to digest for three weeks before being filtered onto a $10 \mu m$ polycarbonate filter membrane. Solids left from filtration were then transferred to a 10% H_2O_2 solution for three weeks to remove residual organic matter. Finally, the solution was filtered using a $10 \mu m$ polycarbonate filter membrane, followed by manual isolation of individual microplastics using tweezers and a microscope. 348 microparticle debris samples were collected

2.2. Raman Spectra Collection

A 785nm laser (785nm laser: Innovative Photonics Solution IO785MM0350M64F) is focused onto the sample by a microscope (Olympus BX-51) fitted with a high magnification objective (Reichert Plan Achromat 40x / 0.17NA Infinity Objective). Raman scattered light enters a Spectrometer (Princeton Instruments Acton SP2300) with grating (600 grooves/mm with 4.5 cm⁻¹ resolution) and collected on a CCD camera (Princeton Instruments PIXIS-100 CCD) using Lightfield software. An aluminum substrate was used to provide a neutral background during sample collection. Due to the small cross-section of the collected fibers,

it was necessary to use a high magnification(40x) objective and long exposure times (30s) to collect an adequately strong signal.

2.3. Reference Library of Known Materials

Spectra of 18 known materials were collected in the range 400-3000 cm⁻¹ for use as a spectral library. In addition to the in-house collected spectra, our reference library also includes the publicly available SLoPP and SLoPP-E microplastic Raman database,²⁰ which contains Raman spectra from plastics and other materials commonly found in the environment. In total, our reference library contains 278 unique spectra from 28 unique materials.

2.4. Data Processing: Resampling

Raman spectra from our in-lab-collected samples and external samples are wavenumber-calibrated using a resampling algorithm written in Python. First, linearly spaced wavenumber values of zero value are inserted into a spectrum. A wavenumber resolution of 1 cm⁻¹ was used for simplicity. Next, intensities for the newly created wavenumbers were calculated by interpolation of the original spectral data while accounting for the distance between the new data point and the nearest neighbors. The spectrum is then re-indexed to include only the regularly spaced wavenumbers at intervals of 1 cm⁻¹. Finally, the spectrum is truncated to obtain universally consistent endpoints. The resulting wavenumber range is 402-1990 cm⁻¹. This range was chosen empirically based on the ranges of available library spectra.

2.5. Data Processing: Peak Isolation

Peaks of interest in the sample spectra were isolated from the background using a gradient-based peak isolation algorithm followed by normalization. The peak isolation algorithm proceeds as follows for one spectrum. The first 49 datapoint are set equal to the 50th point. This flattens the leading data to minimize boundary effects. Next, A discrete wavelet trans-

form (DWT) using the ‘sym5’ wavelet removes the first three high frequency decompositions from the spectrum. This step minimizes system-to-system variations in the fixed-pattern noise from different spectrometers. Next, A DWT-based iterative background estimation²¹ removes the fluorescence contribution from the spectrum. Ten iterations of level seven DWT decomposition sufficiently estimate and removes the broad background fluorescence. The spectral peaks are then isolated by computing the second derivative of the spectrum. Finally, L2 normalization and mean centering are performed on the spectrum.

2.6. Matching Spectra

Spectral matches are scored by calculating the vector angle between two spectra using the dot product (Eqn. 1). A threshold value of 1 was used to distinguish between a good match and a poor match. The signal to noise ratio of each spectra were calculated using Equation 2. False positives caused by a weak signal were removed using a signal to noise ratio threshold of 10.

3. Results & Discussion

3.1. Efficacy of the Matching Algorithm

The matching algorithm described above uses the dot product (Eqn. 1) to find the best match to a spectrum in the reference library. Additionally, considering the signal to noise ratio (Eqn. 2) identifies false positives and helps account for the absence of a match.

When a sample attains a good match score (<1) and exhibits a good signal to noise ratio (>10) we consider it a Great match (Fig 2a). This example shows the ideal situation where a marine litter samples matches almost exactly to a sample found in the library.

A few spectra gave an anomalous result of a good match score despite having a low SNR (Fig 2b). We characterized these samples Error because despite closely matching to a spectrum in the library the SNR fell below the acceptable limits of a meaningful signal. We treat such cases as false positives and do not count them in the list of positive identifications.

A sample that receive a Match Score greater then 1 count as unidentified. These samples fall into one of two categories: No Raman Signal (Fig 2c) and Expand Library (Fig 2d). If the SNR is below the threshold then the signal is too weak to be meaningful and labeled No Raman Signal. The algorith, calls for a new measurement, however that was not done for this study. Spectra with good SNR (>10) but a poor match score (>1) signify a need to expand the library. We label these as Expand Library and call for the collection of more reference spectra to positively identify these samples. Spectra in this category also showed a lower average SNR than spectra with good matches. This suggests that obtaining a good Raman signal for each sample is crucial for correct identification. The number of samples in each category are shown in Table 1a.

Three databases were used to provide a library of reference spectra to calculate best spectral matches (Grant, SLoPP, SLoPP-E). The proportion of Great matches made from each database are shown in Table 1b. The Grant Lab Database contains 18 reference spectra

(6.4% of the full library) yet produced about half of the positive matches. This disproportion is primarily due to the raw signal similarity of spectra collected on the same spectrometer. The spectra obtained from the third party database have undergone postprocessing steps such as baseline correction, cosmic ray removal and smoothing prior to our own postprocessing routine. While importing spectra they are all processed using the same algorithm, which may cause a distortion of the doubly processed external library. This causes the third party library to perform less efficiently than the library built in our own lab, which is exemplified in the lower average match score of the internal Grant Lab reference library compared to the external SLoPP and SLoPP-E libraries. Despite the external libraries providing less matches proportionally, it can be seen in Fig. 2 A that the post processing routine does indeed provide excellent matches on external reference spectra.

Table 1

Type of Match	n	Percent	Database	n	Avg. Match Score	
Good Match	199	57.2%	Grant Lab	93	0.57	
Expand Library	87	25.0%	SLoPP	98	0.81	
No Raman Signal	60	17.2%	SLoPP-E	8	0.68	
Error	2	0.6%	B. Quantity of each Positive match sourced from each database			
A. Distribution of each type of match						

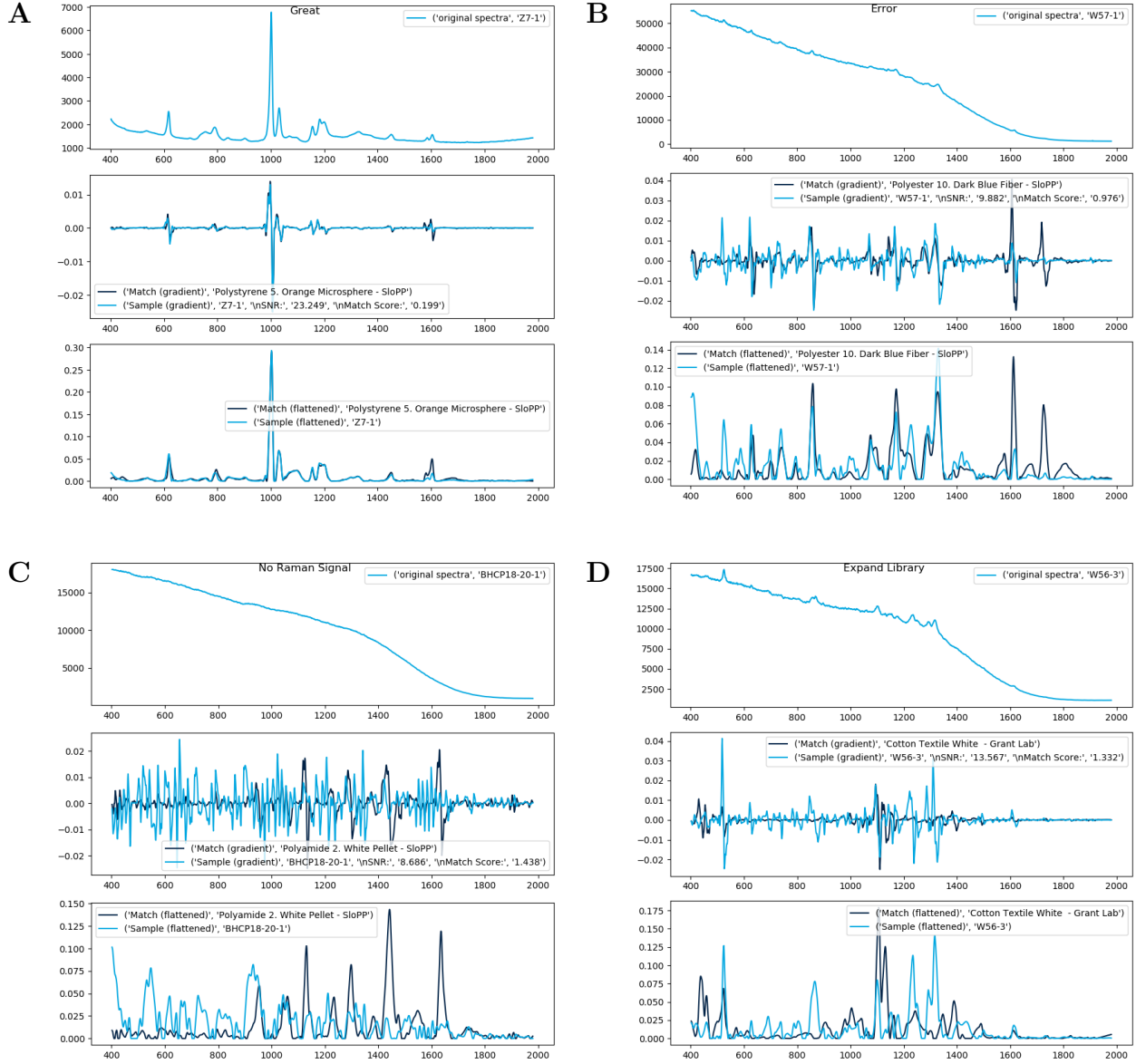


Figure 2: Representative examples of each type of match. A) Great, B) Error, C) Expand Library, D) No Raman Signal. Each subfigure contains a triplicate of processed spectra: The raw spectra (top) after resampling, the second derivative of the corrected spectra (middle), which is used for matching, and the zero-background spectra (bottom), which is used as a visual aid familiar to researchers.

3.2. Material Identification

Proportions of identified plastic, non-plastic and unidentified samples are shown in Table 2a. 25.9% of all samples were positively identified as being composed of synthetic polymeric material. Non-plastics made up 31.3% of all samples. The large number of non-plastics highlights the need for microplastics research to incorporate some form of chemical identification to accurately assess the true level of microplastic contamination in the environment. It is impossible to distinguish between anthropogenic and natural debris on the micro scale by imaging experiments alone. 42.8% of all samples did not meet the matching criteria. This is due in part to an incomplete library. It is impossible to generate a complete library of reference spectra of every type of plastic including chemical modifications, dyes, environmental damage, etc. However, obtaining more reference spectra is necessary to increase the positive match rate. This finding also illustrates the need for a robust, publicly available library of microplastic reference spectra. Even with a library of over 500 spectra almost half were unidentifiable due in part to an incomplete library. Another contribution to the large number of unidentifiable spectra is a weak Raman signal during collection. The small cross sections of the fibers make it difficult to obtain a strong signal with high signal to noise ratio. Proper care must be taken to ensure sample spectra have an adequate signal.

Table 2: Proportion of materials identified by Raman

Material Category	n	Percent	Plastic Type	n	Percent
Plastic	90	25.9%	Polyester	56	62.2%
Non-Plastic	109	31.3%	Polyethylene Terephthalate	14	15.6%
Unidentified	149	42.8%	Rayon	4	4.4%
A. Material Catergory					
B. Non-Plastics					
Non-Plastic	n	Percent	C. Plastics		
Cotton	70	64.2%	Polyamide	3	3.3%
Cellulose (Natural)	37	33.9%	Polyethylene	3	3.3%
Wool	2	1.8%	Polypropylene	3	3.3%

The proportion of positively identified plastics are shown in Table 2c. The overwhelming majority of positively identified plastics were composed of Polyester and Polyethylene Terephthalate. While there are many types of polyesters, the most common is Polyethylene Terephthalate, so these two categories could reasonably be considered as one: PET. The reason for the difference in categorization is how the source material for the reference spectra was labelled. The Library entry for Polyester was sourced from clothing fibers whose tags indicated “Polyester” as the garment material. The Library entry for PET was sourced from Packaging materials labelled as PET. Their polymer composition may be nearly identical, but the library entries for polyester may also include a contribution of the signal from dyes in the material. Many of the common names for plastics will overlap with the chemically named counterpart. For instance, Rayon is composed of cellulose and Nylon is the name for one of the most popular polyamide. These overlaps should be considered when interpreting micro-plastics data. Another interesting result of this experiment is that the number of cellulose acetate debris samples is very low relative to PET. Cellulose acetate is the material that cigarette butts are made of and if visible litter on the street were proportional to levels of marine litter, one would expect to find a high level of cellulose acetate fibers in the ocean. However, cellulose acetate is readily biodegradable and decomposes within months,

where plastic microfibers like PET are a much more persistent pollutants, contaminating the marine environment for decades. Furthermore, the potassium hydroxide digestion used for microplastics purification has been shown to partially degrade cellulose acetate,²² which may lead to lower number of cellulose acetate particles in the final results.

Positively identified non-plastics are listed in Table 2b. Almost all non-plastic samples were matched with either Cotton or natural Cellulose derived from wood pulp. Cotton is primarily composed of cellulose so these two categories may be grouped together as cellulose under some interpretations. It has been found that clothing fibers are a major source of microplastics so it is unsurprising to find cotton fibers as a major component in the tested samples. Although natural fibers such as cellulose are not considered a serious threat to the environment, their inclusion in the library is important for properly distinguishing between plastic and non-plastics particles. This is especially true for extremely small samples that can not be identified by eye.

4. Conclusion and Future Work

The algorithm described in this report offers a robust system that can quickly identify microplastics and cellulosic fibers isolated from natural environments. Moreover, The large size of the library and the multitude of spectra for each material allow for proper identification of environmentally damaged materials. About 57% of samples were positively identified by their spectra, while the remaining samples were left unidentified. One quarter of the samples were unidentified because there was not a good match found in the library. Improving this metric would require a larger library containing more materials. 17.2% of samples were unidentified because their Raman signal was too weak to find a proper match. This problem is best overcome by obtaining stronger signals with longer acquisition times.

It was previously mentioned that one major barrier to microplastics research is the laborious nature of sample collection, isolation and identification. The work described in this paper has addressed the need for rapid chemical identification of pre-sorted samples. This leaves much room for innovation in the isolation of samples as well as their morphological identification. The major data-collection bottlenecks in this study were the particle-by-particle isolation of individual suspected microplastics, and the particle-by-particle Raman spectrum acquisition. Each of these steps took several weeks, causing a serious hindrance to progress in the field. Future work on this project will focus on improved efficiency and automation of these time consuming steps.

The automation and rapid measurement of micro and nanoplastic sizes would be a huge improvement to the current workflow. Nanoparticle Tracking Analysis (NTA) allows for the expeditious measurement of individual particles in the micro to nano size regime and may work well for micro and nanoplastics, especially when used in conjunction with Interferometric Scattering Microscopy (iSCAT) and a robust software suite. iSCAT is a relatively new and underutilized optical technique that can detect particles in solution far below the diffraction limit. A schematic of a typical iSCAT system is shown in Figure 3. A scat-

tering object illuminated by a coherent light source is imaged as a point spread function. The amplitude of the point spread function (pixel value) can be calibrated to the mass of the scattering object, allowing for particle-by-particle measurement of analyte mass. This system has been built and used to image 15nm gold nanoparticles (AuNP's) as shown in Figure 4. Future work will use this system to image nanoplastics. Particle tracking is also being implemented into the iSCAT system (Fig. 5), turning it into a nanoparticle tracking analyzer. Total particle counts as well as darkest pixel value are recorded in real-time. This system would greatly enhance throughput when counting and measuring the size of micro and nanoplastics.

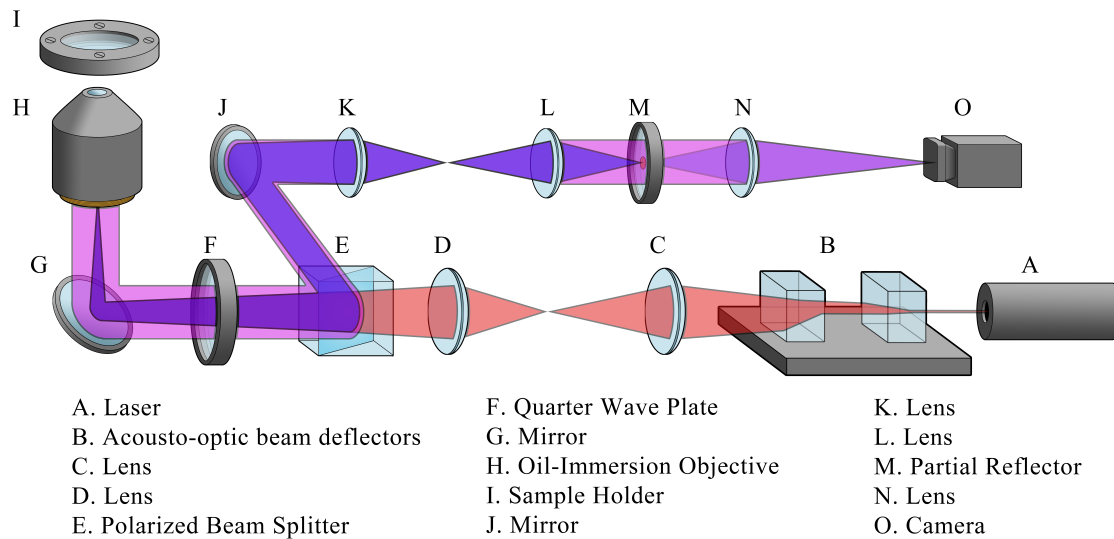


Figure 3: Diagram of an Interferometric Scattering Microscope

Combining iSCAT with Raman may offer a promising method for obtaining chemical and morphological information simultaneously. Surface Enhanced Raman Spectroscopy has been shown as promising avenue for chemical identification of micro and nanoplastics.²³ In this study, silver nanoparticles adsorbed onto micro and nano plastics ranging in size from 100nm to 10 μ m enhanced the Raman spectrum. The SERS effect of the silver nanoparticles enabled the detection of small cross section nanoplastics. Incorporating a SERS component into an iSCAT based NTA would allow for the simultaneous acquisition of micro and nanoplastic quantity, size, and chemical composition. These improvements are expected to

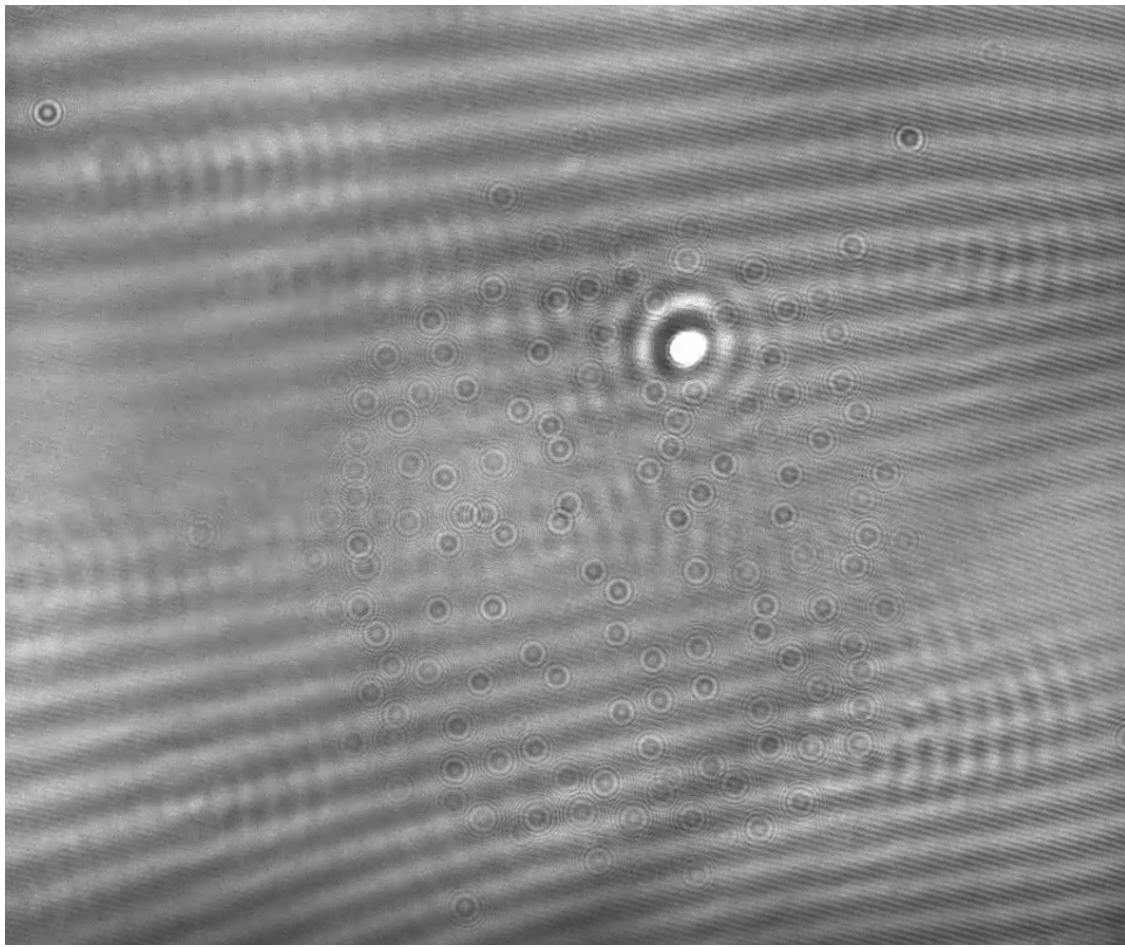


Figure 4: 15nm Gold Nanoparticle imaged by iSCAT system

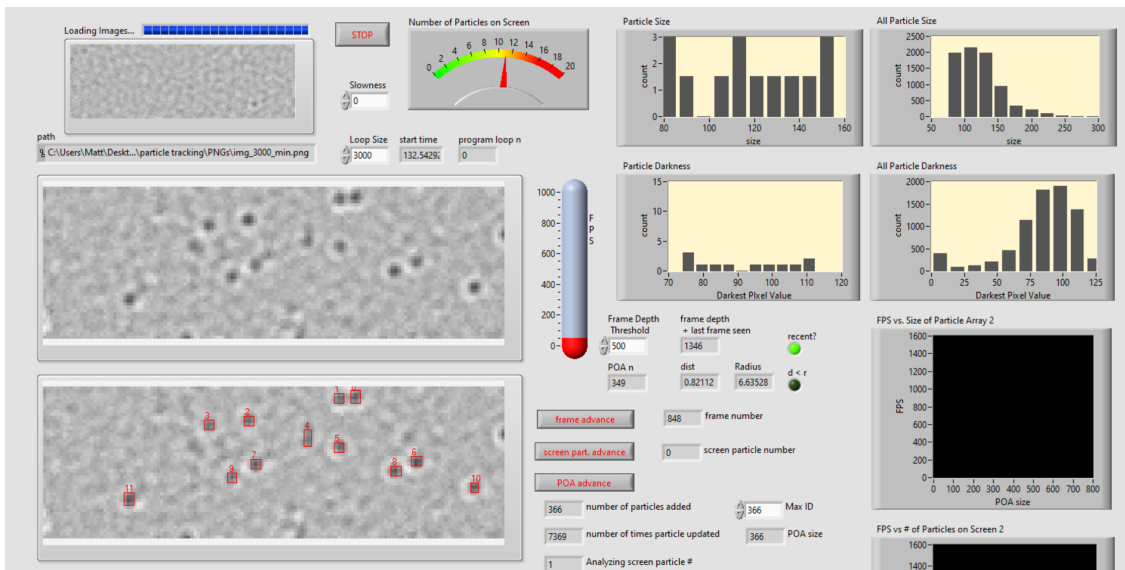


Figure 5: Particle Tracking Software

make microplastics research both easier and faster than methods currently in use.

5. Bibliography

- (1) Geyer, R.; Jambeck, J. R.; Law, K. L. Production, use, and fate of all plastics ever made. *Science Advances* **2017**, 3.
- (2) Kimberly Ann V.Zubris, B. K. Synthetic fibers as an indicator of land application of sludge. *Environmental Pollution* **2005**, 138, 201–211.
- (3) G.S.Zhang, Y. The distribution of microplastics in soil aggregate fractions in south-western China. *Science of The Total Environment* **2018**, 642, 12–20.
- (4) Allen, S.; Allen, D.; Moss, K.; Le Roux, G.; Phoenix, V. R.; Sonke, J. E. Examination of the ocean as a source for atmospheric microplastics. *PLOS ONE* **2020**, 15, 1–14.
- (5) Al-Sid-Cheikh, M.; Rowland, S. J.; Stevenson, K.; Rouleau, C.; Henry, T. B.; Thompson, R. C. Uptake, whole-body distribution, and depuration of nanoplastics by the scallop *Pecten maximus* at environmentally realistic concentrations. *Environmental science & technology* **2018**, 52, 14480–14486.
- (6) Lisbeth Van Cauwenberghe, C. R. Microplastics in bivalves cultured for human consumption. *Environmental Pollution* **2014**, 193, 65–70.
- (7) Oßmann, B. E.; Sarau, G.; Holtmannspötter, H.; Pischetsrieder, M.; Christiansen, S. H.; Dicke, W. Small-sized microplastics and pigmented particles in bottled mineral water. *Water research* **2018**, 141, 307–316.
- (8) Zalasiewicz, J.; Waters, C. N.; Ivar do Sul, J. A.; Corcoran, P. L.; Barnosky, A. D.; Cearreta, A.; Edgeworth, M.; Galuszka, A.; Jeandel, C.; Leinfelder, R. et al. The geological cycle of plastics and their use as a stratigraphic indicator of the Anthropocene. *Anthropocene* **2016**, 13, 4–17.

- (9) Gregory, M. R. Virgin plastic granules on some beaches of eastern Canada and Bermuda. *Marine Environmental Research* **1983**, 10, 73–92.
- (10) Bakir A, T. R., Rowland SJ Enhanced desorption of persistent organic pollutants from microplastics under simulated physiological conditions. *Environ Pollution* **2014**, 185, 16–23.
- (11) Cedervall T, e. a., Hansson L.A. Food Chain Transport of Nanoparticles Affects Behaviour and Fat Metabolism in Fish. *PLOS ONE* **2012**, 7.
- (12) Arthur, C.; Baker, J.; Bamford, H. Proceedings of the international research workshop on the occurrence, effects and fate of microplastic marine debris. *NOAA Technical Memorandum* **2009**,
- (13) Klaine, S. J.; Koelmans, A. A.; Horne, N.; Carley, S.; Handy, R. D.; Kapustka, L.; Nowack, B.; von der Kammer, F. Paradigms to assess the environmental impact of manufactured nanomaterials. *Environmental Toxicology and Chemistry* **2012**, 31, 3–14.
- (14) De Falco, F.; Cocca, M.; Avella, M.; Thompson, R. C. Microfiber Release to Water, Via Laundering, and to Air, via Everyday Use: A Comparison between Polyester Clothing with Differing Textile Parameters. *Environmental Science and Technology* **2020**, 54, 3288–3296.
- (15) Efimova, I.; Bagaeva, M.; Bagaev, A.; Kilesso, A.; Chubarenko, I. P. Secondary Microplastics Generation in the Sea Swash Zone With Coarse Bottom Sediments: Laboratory Experiments. *Frontiers in Marine Science* **2018**, 5, 313.
- (16) Dawson, A. L.; Kawaguchi, S.; King, C. K.; Townsend, K. A.; King, R.; Huston, W. M.; Bengtson Nash, S. M. Turning microplastics into nanoplastics through digestive fragmentation by Antarctic krill. *Nature Communications* **2018**, 9, 1–8.

- (17) Eriksen, M.; Lebreton, L. C. M.; Carson, H. S.; Thiel, M.; Moore, C. J.; Borerro, J. C.; Galgani, F.; Ryan, P. G.; Reisser, J. Plastic Pollution in the World's Oceans: More than 5 Trillion Plastic Pieces Weighing over 250,000 Tons Afloat at Sea. *PLOS ONE* **2014**, 9, 1–15.
- (18) Hernandez, L. M.; Yousefi, N.; Tufenkji, N. Are there nanoplastics in your personal care products? *Environmental Science & Technology Letters* **2017**, 4, 280–285.
- (19) Oliveri Conti, G.; Ferrante, M.; Banni, M.; Favara, C.; Nicolosi, I.; Cristaldi, A.; Fiore, M.; Zuccarello, P. Micro- and nano-plastics in edible fruit and vegetables. The first diet risks assessment for the general population. *Environmental Research* **2020**, 187, 109677.
- (20) Munno, K.; De Frond, H.; O'Donnell, B.; Rochman, C. M. Increasing the accessibility for characterizing microplastics: Introducing new application-based and spectral libraries of plastic particles (SLoPP and SLoPP-E). *Analytical Chemistry* **2020**, 92, 2443–2451.
- (21) Galloway, C.; Le Ru, E.; Etchegoin, P. An iterative algorithm for background removal in spectroscopy by wavelet transforms. *Applied Spectroscopy* **2009**, 63, 1370–1376.
- (22) Alexandre Dehaut, L. F. L. H. C. H. E. R. G. R. C. L. P. S. A. H. G. D. I. P.-P., Anne-Laure Cassone Microplastics in seafood: Benchmark protocol for their extraction and characterization. *Environmental Pollution* **2016**, 215, 223–233.
- (23) Lv, L.; He, L.; Jiang, S.; Chen, J.; Zhou, C.; Qu, J.; Lu, Y.; Hong, P.; Sun, S.; Li, C. In situ surface-enhanced Raman spectroscopy for detecting microplastics and nanoplastics in aquatic environments. *Science of the Total Environment* **2020**, 728, 138449.